

Controls on schwertmannite transformation rates and products

Klaus-Holger Knorr, Christian Blodau *

Limnological Research Station and Department of Hydrology, University of Bayreuth, D-95440 Bayreuth, Germany

Received 2 December 2006; accepted 27 April 2007

Editorial handling by B. Kimball

Available online 25 May 2007

Abstract

To study the impact of geochemical conditions on the fate of schwertmannite in AMD polluted sediments, pH, concentrations of SO_4^{2-} and DOC, and temperature were varied in batch experiments. Schwertmannite transformation was quantified by titration of released acidity and the product investigated with FTIR, XRD, SEM/EDX, and chemical extraction. Rates ranged from 0.0002 d^{-1} to 0.13 d^{-1} (transformed fraction/incubation time). Raising pH from 3 to 5 increased transformation by a factor of $5.8 (\pm 2.1)$ and temperature from 10 to 20°C by a factor $3.8 (\pm 1.6)$. Sulphate (20 mmol L^{-1}) and DOC (20 mg L^{-1}) lowered transformation by a factor of $2.5 (\pm 0.4)$ and $2.4 (\pm 0.5)$, respectively. The Fe phase was less dissolvable in 1 N HCl but goethite was not detected by XRD. The morphology changed little, even in SO_4^{2-} -poor Fe phases. An amorphous, SO_4 depleted Fe phase thus formed. Most of the SO_4 released from the schwertmannite tunnel structure remained within this phase but changes in IR bands at 1108 cm^{-1} (ν_3) and 984 cm^{-1} (ν_1) suggested a relocation of SO_4 . The study documents the high potential of schwertmannite to buffer pH increase in sediments, particularly at low SO_4^{2-} concentrations, and high temperatures.

© 2007 Elsevier Ltd. All rights reserved.

1. Introduction

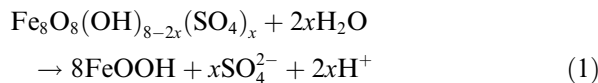
The formation and transformation of schwertmannite is of geochemical significance in surface waters polluted with acid mine drainage (AMD) (e.g. Blodau and Peiffer, 2003; Kuesel, 2003; Peine et al., 2000; Regenspurg et al., 2004). Schwertmannite is an iron(III)-oxyhydroxysulphate with the general formula $\text{Fe}_8\text{O}_8(\text{OH})_{8-2x}(\text{SO}_4)_x$ and $1 \leq x \leq 1.75$ (Bigham et al., 1990). The mineral is formed in the

presence of high SO_4^{2-} concentrations at pH values between 2.5 and 4.5 (Bigham et al., 1994; Yu et al., 1999). While first a tunnel structure akin to that of akaganéite (β -FeOOH) was proposed, having distorted SO_4^{2-} tetrahedrons within the tunnels instead of Cl^- (Bigham et al., 1990), its structure is again under debate and not yet clarified (Majzlan and Myneni, 2005; Waychunas et al., 2001).

In many AMD polluted lakes, the uppermost layers of the sediment mainly consist of schwertmannite (Regenspurg et al., 2004). From batch experiments and mineralogical change with burial in sediments it was inferred that schwertmannite hydrolyzes to form goethite (α -FeOOH) (Bigham et al., 1990, 1996b) (Eq. (1)).

* Corresponding author. Tel.: +49 921 552223; fax: +49 921 552049.

E-mail address: christian.blodau@uni-bayreuth.de (C. Blodau).



Sediments rich in schwertmannite therefore often acidify to a pH around 3 due to the buffering effect of schwertmannite transformation (Blodau, 2004; Peine et al., 2000). This effect is of significance because acidification impedes SO_4^{2-} reducing bacteria but promotes Fe reducing bacteria (Blodau and Peiffer, 2003; Kuesel, 2003). If Fe reduction is the predominant electron accepting process in the sediments, Fe(II) is mobilized and may cause further acidification in the surface waters by reoxidation to Fe(III) and precipitation as schwertmannite (Peine et al., 2000).

The solubility and stability constants of schwertmannite have previously been determined (Bigham et al., 1996b; Kawano and Tomita, 2001; Majzlan et al., 2004; Yu et al., 1999). Less is known about the factors controlling schwertmannite transformation rates. Schwertmann and Carlson (2005) documented increasing transformation rates with increasing pH, and a complete transformation to goethite in deionized water within ~ 100 days. A transformation time of > 514 days was reported for natural samples incubated in original pore water (Jonsson et al., 2005). An inhibiting effect of SO_4^{2-} on transformation rates was mentioned by Bigham et al. (1996b) but the authors did not provide quantitative data. Jonsson et al. (2005) reported a preservation of schwertmannite at low temperature. They found that schwertmannite did not transform for more than 5 years at a pH of ~ 3 and a temperature of 4°C . Blodau (2004) found an Fe phase with properties characteristic of schwertmannite to be stable at $\text{pH} > 5$ in sediments of an acidic mine lake. In other sediments with a pH of about 3, schwertmannite was transformed to goethite in periods of several years (Peine et al., 2000). The transformability of schwertmannite may, therefore, greatly vary in AMD polluted environments, and more information is needed about the stability of the mineral under varying geochemical conditions.

To identify controls on schwertmannite stability, we investigated transformation rates and products in batch experiments. Temperature, pH, sulphate, and DOC concentration were varied. Transformation rates were determined by titration and the mineralogical nature of the formed products was investigated.

2. Materials and methods

2.1. Mineral synthesis

Schwertmannite and goethite were synthesized following Bigham et al. (1990) and Cornell and Schwertmann (1996), respectively, and identified by XRD and FTIR. Based on the Fe and S content, an average stoichiometry of $\text{Fe}_8\text{O}_8(\text{OH})_{5.4}(\text{SO}_4)_{1.3}$ was calculated for the synthetic schwertmannite (Regenspurg et al., 2004). The BET surface area was $51 \text{ m}^2 \text{ g}^{-1}$ for goethite and $177.5 \text{ m}^2 \text{ g}^{-1}$ for schwertmannite.

2.2. Treatments and analytical methods

The solutions for the experiments were based on natural analogues in AMD polluted waters (Blodau, 2004; Peine et al., 2000). They contained Ca (5 mM), K (1 mM), Mg (2 mM), NH_4 (0.3 mM), Al (0.1 mM), Na (2 or 26 mM), SO_4^{2-} (1 or 20 mM), Cl^- (charge balance) and DOC (0 or 20 mg L^{-1}). DOC stemmed from a sterilized leaf litter extract (see electronic supplementary material) and was measured using a TOC analyzer (Shimadzu). No detectable change was found in DOC during the incubation (standard deviation of measurements $\sim 0.5 \text{ mg L}^{-1}$). To $\sim 0.2 \text{ g}$ of schwertmannite 100 mL of solution was added. The pH was adjusted to 3 or 5 using 6 M HCl, and checked with a glass electrode (WTW). The solution was placed in the dark at constant temperature of either 20°C ($\pm 1^\circ\text{C}$) or 10°C , and shaken occasionally. Based on previous studies an incubation time of ~ 100 days was chosen to ensure partial transformation, but to avoid complete transformation. For adjustment of pH 0.05 N NaOH and a titration apparatus (Titribo, Metrohm AG, Switzerland) was used. For the measurement, a previously calibrated electrode was inserted and removed after titration was completed. Sodium hydroxide consumption was converted into a schwertmannite transformation according to the stoichiometry of $\text{Fe}_8\text{O}_8(\text{OH})_{5.4}(\text{SO}_4)_{1.3}$. Sulphate concentrations were measured on a 0.5 mL aliquot using ion chromatography (Metrohm IC, METROSEP Anion Dual 3 column, chemical suppression). It was ensured that sampling and titration did not change the volume of solution by more than 5%.

After 109 days, the solution was decanted and the solid phase rinsed twice with 'fresh' incubation

solution before analysis of the solid phase. Reactive Fe was extracted from 0.1 g freeze dried sample for 24 h using 20 mL of 1 M-HCl (Wallmann et al., 1993) and determined by atomic absorption spectroscopy (AAS). Freeze dried samples were X-rayed on glass slides between 2° and 80° 2θ (Bruker D5000 XRD, Co K α radiation) and identified using the mineral library of the Diffrac-AT software (Version 3.2, 1994) provided with the instrument and data from Cornell and Schertmann (1996). For characteristic 2θ values see electronic supplementary material, Table 3S. Scanning electron micrographs were recorded using a Keo 1530 Gemini SEM (Schottky cathode, current \sim 250 pA) equipped with an EDX system (Inca, Oxford Instruments). Sulphate bonding to schertmannite was investigated with FTIR spectroscopy. IR spectra were recorded on a Bruker Vektor 22 FTIR Spectrometer using the KBr-pellet technique (see electronic supplementary material). Surface areas (BET, Kr) of post-treatment samples were recorded for a pooled sample with complete (10/20 °C, pH 5, 1 mM SO₄) and a sample with partial (20 °C, pH 5, 20 mM SO₄) transformation of schertmannite. Samples were dried at 105 °C (vacuum) and measured on an ASAP 2020-KRYPTON analyzer.

Schertmannite transformation rates were calculated by dividing the transformed fraction by the corresponding time interval. Details about mineral synthesis, the DOC preparation, XRD, SEM and FTIR measurements are provided in the electronic supplementary material.

3. Results

3.1. Schertmannite transformation rates

Protons were continuously and uniformly released in treatments at pH 3, equivalent to transformation rates of 0.0002 d⁻¹–0.0030 d⁻¹. At pH 5, the release was initially much faster than at pH 3 (Fig. 1), with rates ranging from 0.13 d⁻¹ to 0.32 d⁻¹ in the first 10 days, but decreased to a similar magnitude (0.0004 d⁻¹–0.0045 d⁻¹; Table 1 bottom). This decrease was stronger than a simple first order exponential decay of schertmannite. Transformation thus impeded itself after some time. At low SO₄²⁻ concentrations, nearly all of the schertmannite was transformed in 109 days according to the H⁺ release and the stoichiometry of the initial schertmannite.

Transformation was most strongly affected by pH (Table 1, Fig. 1). A pH increase from 3 to 5 raised transformation rates by a factor of 1.4 (high SO₄²⁻, 20 °C) to 13.9 (low SO₄²⁻, 10 °C). Overall, transformation rates were increased by a factor of 5.8 ± 2.1. A temperature increase of 10 °C raised rates by a factor of 2–10 at pH 3, and by a factor 1.2–1.5 at pH 5. On average, rates increased by a factor of 3.8 ± 1.6 per 10 °C. High SO₄²⁻ and DOC concentrations lowered the transformation at all temperatures and pH values by a factor of 1.3 to >3 (Table 1). On average, transformation was lowered by a factor of 2.5 ± 0.4 (SO₄²⁻) and 2.4 ± 0.5 (DOC). The impact of changes in experimental conditions thus decreased in the order pH > T > [SO₄²⁻] ≈ [DOC].

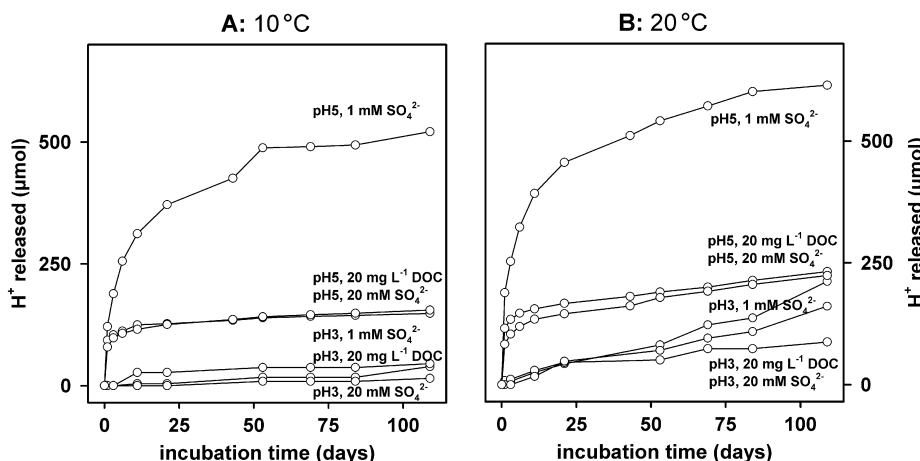


Fig. 1. H⁺ released during the incubation experiment. Results for 10 °C are given in A, and for 20 °C in B.

Table 1

Schwertmannite transformation percentages (top) and rates (bottom) estimated by titrated acidity release

Transformation of schwertmannite (titration)	10 °C incubation		20 °C incubation	
	pH 3%	pH 5%	pH 3%	pH 5%
SO ₄ ²⁻ 1 mmol L ⁻¹	5.8	80.9	33.6	102.7
SO ₄ ²⁻ 20 mmol L ⁻¹	2.3	25.2	25.1	34.0
DOC 20 mg L ⁻¹	7.2	23.9	13.8	37.2
Transformation rates calculated from titration	10 °C incubation		20 °C incubation	
	pH 3 (d ⁻¹)	pH 5 ^a (d ⁻¹)	pH 3 (d ⁻¹)	pH ^a (d ⁻¹)
SO ₄ ²⁻ 1 mmol L ⁻¹	5.28×10^{-4}	1.88×10^{-1} 1.96×10^{-3}	3.14×10^{-3}	3.15×10^{-1} 4.54×10^{-3}
SO ₄ ²⁻ 20 mmol L ⁻¹	2.16×10^{-4}	1.29×10^{-1} 7.38×10^{-4}	2.58×10^{-3}	1.26×10^{-1} 1.53×10^{-3}
DOC 20 mg L ⁻¹	3.04×10^{-4}	1.50×10^{-1} 4.15×10^{-4}	1.93×10^{-3}	1.85×10^{-1} 1.32×10^{-3}

^a Initial and transformation rates after 20–40 d.

Concentration changes of SO₄²⁻ in solution could only be detected in the SO₄²⁻ poor treatments. At pH 3, SO₄²⁻ concentrations slightly decreased ($-0.22 \text{ mmol L}^{-1} \pm 0.20$), whereas at pH 5 they slightly increased ($+0.18 \text{ mmol L}^{-1} \pm 0.16$). This was equivalent to a mean uptake of $22 \pm 20 \mu\text{mol}$ ($\sim 5.3\%$) into the solid phase (pH 3), or a mean release of only $18 \pm 16 \mu\text{mol}$ ($\sim 4.3\%$) (pH 5).

3.2. Transformation products

The characterization of the solid phase confirmed that schwertmannite was transformed. The content of 1 M HCl dissolvable Fe was lowered from $85 \pm 0.9\%$ (initial schwertmannite) to 55–26% (Table 1S, electronic supplementary material), indicating increasing crystallinity of the Fe phase. The broad diffraction peaks of schwertmannite were still present in samples with moderate transformation rates (Table 1) and diminished in the other treatments (Fig. 2). Goethite, however, was not detectable by XRD in any sample (Fig. 2). The sharp diffraction peaks at 24.12° , 36.32° and 36.97° , as well as almost all weaker peaks, can be attributed to gypsum and halite that formed during freeze drying of the samples. The diffraction patterns were also examined for jarosite, akaganéite, and alunite, but neither these nor any further mineral phases could be identified. The diffraction results thus indicate that the formation of goethite was impeded, and that an X-ray amorphous product developed.

The SEM micrographs revealed that – apart from the development of gypsum or halite needles – the transformation process did not substantially change

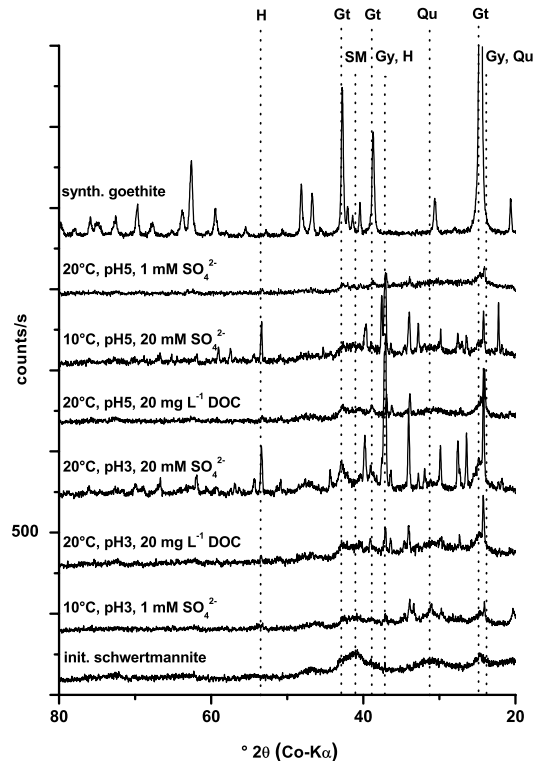


Fig. 2. X-ray diffraction patterns of synthetic schwertmannite, goethite and selected samples. The y-axis scale is identical for all diffractograms. Peaks indicative of relevant minerals are marked with dotted lines (H: halite, Gt: goethite, SM: schwertmannite, Gy: gypsum, Qu: quartz). For other graphs and 2θ values of the minerals see electronic supplementary material.

the morphology of the Fe phase, which remained cloud-like (Fig. 3). An acicular, prismatic morphology typical for goethite was not observed. The ele-

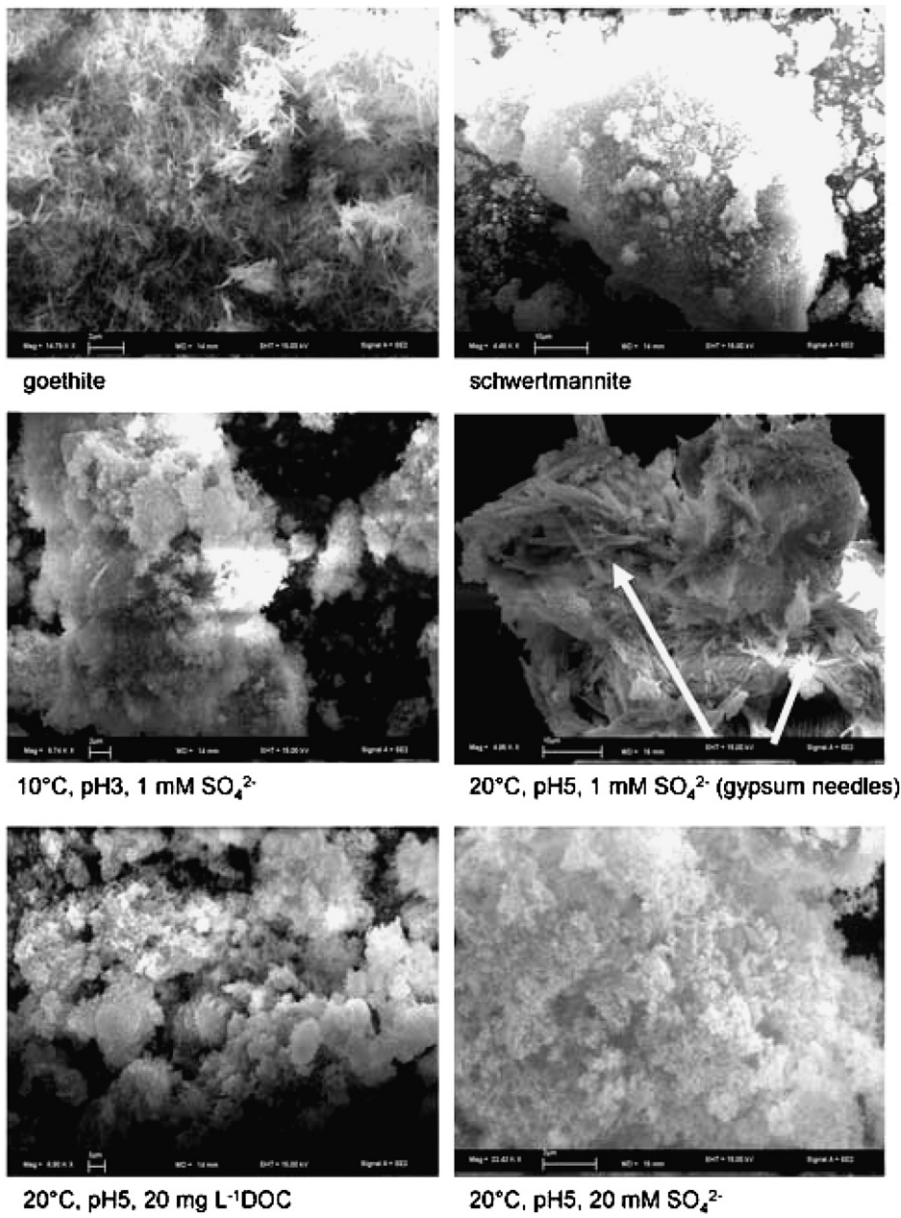


Fig. 3. Scanning electron micrographs of the incubated synthetic schwertmannite, pure synthetic goethite, and selected samples. Gypsum needles observed in [20 °C, pH 5, 1 mM SO₄²⁻] are marked with an arrow. SEM images of all other samples are provided in the [electronic supplementary material](#).

mental composition of the Fe phase, however, was altered. According to the EDX-analysis, S was effectively removed from the Fe phase in samples containing little SO₄²⁻ in solution. Ratios of Fe/S increased from 5.8 (schwertmannite) to 9.6–20.7 (Table 2). In the most strongly transformed samples, individual spots devoid of S were detected (Table 2). The BET (Kr) surface area in the incubated samples was lower than for freshly precipi-

tated schwertmannite (177.5 m² g⁻¹) but did not decrease between a transformation of 34% (91.8 m² g⁻¹) and a transformation of 80–100% (115.2 m² g⁻¹).

Sulphate was not only removed from the Fe phase but likely also relocated, according to FTIR spectra (Fig. 4). An undistorted SO₄²⁻ tetrahedron produces one strong absorption band (ν_3) at about 1108 cm⁻¹. Sulphate bound within the schwertmannite

Table 2
Fe/S ratios derived from EDX and other major elements detected

Sample	Fe/S ratio in micro-aggregates	Other elements
Initial schwertmannite	5.8	–
Goethite	No S	–
10 °C		
pH 3, 1 mM SO ₄ ²⁻	9.6	Cl, Ca
pH 3, 20 mg l ⁻¹ DOC	10.0	Cl, Ca
pH 3, 20 mM SO ₄ ²⁻	2.3	Na, Cl, Ca
pH 5, 1 mM SO ₄ ²⁻	17.8	Na, Cl
pH 5, 20 mg l ⁻¹ DOC	18.8	Cl(Ca)
pH 5, 20 mM SO ₄ ²⁻	2.5	Na, Cl
20 °C		
pH 3, 1 mM SO ₄ ²⁻	11.1	Ca, Na, Cl
pH 3, 20 mg l ⁻¹ DOC	11.8	Cl, Ca
pH 3, 20 mM SO ₄ ²⁻	5.3	Na, Cl, (Ca, Mg)
pH 5, 1 mM SO ₄ ²⁻	20.6/no S	Ca, Cl
pH 5, 20 mg l ⁻¹ DOC	20.7/no S	(Mg)
pH 5, 20 mM SO ₄ ²⁻	2.9/no S	Na, Ca, Cl

Absence of S in individual locations is denoted as “/no S”. Fe/S ratios <5.8 were detected in samples in 20 mM SO₄²⁻ solution, likely because of incomplete rinsing of samples.

nite structure yields a broad and asymmetric ν_3 and an additional ν_1 band at 984 cm⁻¹, indicative of a strongly distorted tetrahedron (Jonsson et al., 2005; Nakamoto, 1997). Sulphate may also form inner sphere complexes with goethite, especially at low pH, yielding similar IR absorption bands as schwertmannite in the range from 1250 to

950 cm⁻¹ (Peak et al., 1999); however, characteristic bands at 795 and 891 cm⁻¹ are also present in this case. Changes in the absorption bands of SO₄²⁻ can thus be interpreted in light of specific binding of SO₄²⁻ to the Fe phase. In samples with a high degree of schwertmannite transformation, ν_3 bands narrowed, the maximum of ν_3 absorption intensity shifted to about 1140 cm⁻¹, and ν_1 bands diminished (Fig. 4A). In samples with a minimum of transformation, ν_3 bands broadened and ν_1 bands became more pronounced (Fig. 4A). With schwertmannite transforming in the experiments, ν_1 bands disappeared and narrowed ν_3 bands were sustained. Sulphate was thus apparently transferred to other locations, leading to less distorted tetrahedrons. This may especially be the case for the 20 °C, pH 5, 1 mM SO₄²⁻ sample (100% transformation), with SO₄²⁻ forming only a weak outer sphere complex with the surface of the new Fe phase. In samples with DOC addition, the ν_3 absorption maximum did not shift to about 1140 cm⁻¹, even at high pH (Fig. 4B). DOC thus apparently inhibited a relocation of SO₄²⁻.

A high degree of transformation calculated from titration was also accompanied by more pronounced peaks at 891 cm⁻¹. This absorption band is also observed for goethite (Cornell and Schwertmann, 1996), but as mentioned above, goethite

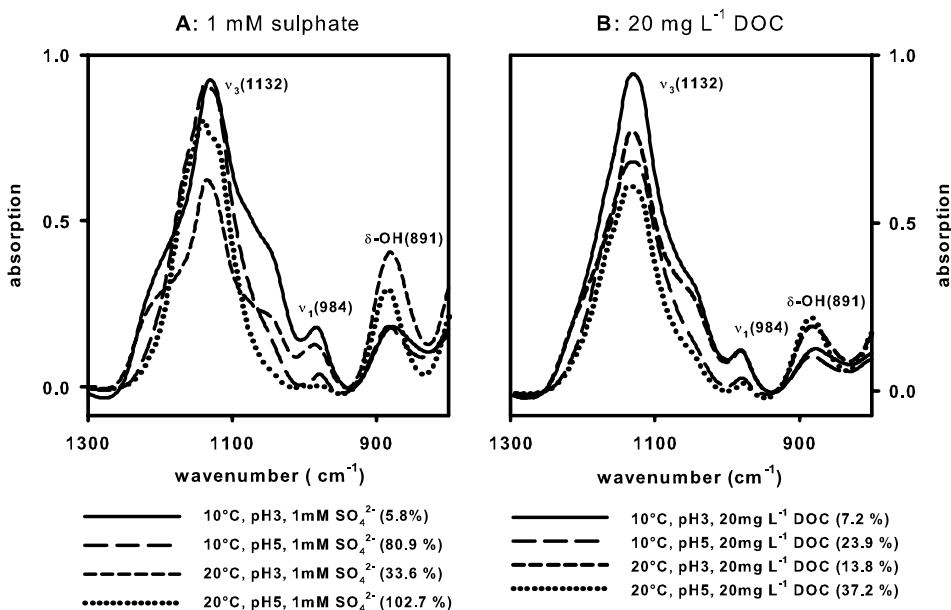


Fig. 4. FTIR spectra of low SO₄²⁻ (A) and high DOC (B) treatments around the 1132 cm⁻¹ ν_3 band. Values in brackets indicate the percentage of schwertmannite transformation according to the titrated acidity. For a description of the 891 cm⁻¹ band see text.

was not detected by XRD. Especially due to the applied KBr technique, this information from changes in FTIR spectra is, however, limited.

4. Discussion

4.1. Schwertmannite transformation rates

Reported rates of schwertmannite transformation have varied by orders of magnitude in batch experiments and sediments (Table 3). It was, for example, documented that the mineral completely transforms within a period of ~100 days in waters of low ionic strength (Schwertmann and Carlson, 2005). The present results at an experimental pH of 5 corroborate this finding (Table 3). In contrast, the mineral appeared to be stable for more than 5 years at a pH of ~3 and a temperature of 4 °C in batch experiments (Jonsson et al.,

2005). Transformation has been reported to occur on a time scale of years in sediments of an acidic mine lake under SO_4^{2-} -rich conditions and a pH of 3–4 (Peine et al., 2000) (Table 3). Much shorter time scales were reported from sediments that were experimentally percolated (Knorr and Blodau, 2006). The factors controlling this variability in transformation rates have not been systematically elucidated yet.

Transformation rates were controlled by pH, temperature, and SO_4^{2-} and DOC concentrations in the experiments. The impact of chemical change decreased in the order $\text{pH} > T > [\text{SO}_4^{2-}] \cong [\text{DOC}]$ (Table 1, Fig. 1). As documented in previous studies (Jonsson et al., 2005; Regenspurg et al., 2004; Schwertmann and Carlson, 2005), pH was thus an important factor controlling the transformation rate. The retardation of schwertmannite transformation by DOC was probably caused by DOC adsorption as

Table 3

Selected transformation rates and geochemical conditions from schwertmannite transformation studies

Transformation rate (d^{-1})	pH	Temp. (°C)	SO_4^{2-} (mmol L^{-1})	DOC (mg L^{-1})	Incubation period (days)	Method	Source
~0	3	4	0–n.d. ^a	0	1825	Titration	Jonsson et al. (2005)
0.0001–0.0004	2–4	n.a. ^a	20–30	n.a.	–	Mass balance	Gagliano et al. (2004) ^b
0.0002	3	10	20	0	109	Titration	This study
0.0003	3.3	~7	~15	~10	–	Mass balance	Peine et al. (2000) ^b
0.0005	3	10	1	0	109	Titration	This study
0.0007	3	10	1	20	109	Titration	This study
0.0013	3	20	1	20	109	Titration	This study
0.0018	4	25	n.d. ^a	0	80	Titration	Schwertmann and Carlson (2005)
0.0018	2.4– 3.9	25	0–2.3	0	547	Titration	Bigham et al. (1996)
0.001 (>0.003)	6	25	0–n.d. ^a	0	514	Titration	Jonsson et al. (2005)
0.002 (>0.005)	9	25	0–n.d. ^a	0	514	Titration	Jonsson et al. (2005)
0.0022 (0.15)	5	10	1	20	109	Titration	This study
0.0023	3	20	20	0	109	Titration	This study
0.0025	5	25	0–n.d. ^a	0	80	Titration	Schwertmann and Carlson (2005)
0.0026	3.3	15	20–27	5–10	95	React iron	Knorr and Blodau (2006)
0.0027	3	25	0–0.8	0	100	SO_4^{2-}	Regenspurg et al. (2004)
0.0031 (0.13)	5	20	20	0	109	Titration	This study
0.0047	7.2	25	0–n.d. ^a	0	95	Titration	Schwertmann and Carlson (2005)
0.0056	5	25	0–0.8	0	28	SO_4^{2-}	Regenspurg et al. (2004)
0.0064	4.6	15	10–15	5–10	95	React iron	Knorr and Blodau (2006)
0.0074	5	10	1	0	109	Titration	This study
0.0092	5	20	1	0	109	Titration	This study

The transformation rate was calculated by dividing the transformed fraction by the corresponding incubation time. Initial rates calculated from the first data points are given in brackets when available.

^a n.a.: not available, n.d.: not detected.

^b Calculated from data in Peine et al. (2000).

previously reported for the transformation of ferrihydrite (Cornell, 1987). The stabilizing effect of SO_4^{2-} was mentioned by Bigham et al. (1996b), and might also occur for other oxoanions, such as arsenate (Fukushi et al., 2003). As expected, the transformation of the mineral accelerated when geochemical conditions differed from those that are most conducive for its precipitation, i.e. millimolar SO_4^{2-} concentrations and pH values between 2.5 and 3.5 (Bigham et al., 1994, 1996a; Yu et al., 1999). However, presence of organic molecules may partly offset increasing instability of the mineral.

Schwertmannite transformation was not only influenced by chemical factors but also strongly temperature dependent, as previously reported by Jonsson et al. (2005). On average, rates increased by a factor 3.8 ± 1.6 per 10°C . The temperature dependency of Fe reduction, which is the primary proton sink in sediments of AMD polluted lakes, is probably lower and on the order of 2.0 per 10°C (Meier et al., 2005). High sediment temperatures during summer may in consequence cause a temporary acidification of pore waters by shifting the proton balance from proton consumption to generation. Indeed, such an effect was observed when temperature was raised from 10°C to 20°C in column experiments (Knorr and Blodau, 2006).

4.2. Transformation products

The release of protons associated with the incorporation of hydroxyl groups into the Fe phase indicated that schwertmannite transformed during incubation (Table 1, Fig. 1). Reactive Fe contents further decreased from initial values of 85% to 26–55%. Therefore, the Fe phase became less accessible to hydrolytic dissolution during the experiment, as would be expected from formation of goethite (Wallmann et al., 1993). A diffraction pattern of goethite did not appear in the samples, however (Fig. 2). This finding departs from the results by Schwertmann and Carlson (2005), who reported an almost complete transformation of schwertmannite into goethite at pH 7 in deionized water within 107 days. IR absorption bands for OH-bending, which are not expressed in pure schwertmannite spectra, appeared at 891 cm^{-1} ($\delta\text{-OH}$) (Fig. 4). This band, among others, may be used for the identification of goethite according to Cornell and Schwertmann (1996), but the intensities remained low and high SO_4^{2-} and DOC concentration levels further

reduced these intensities. The morphology of the initial schwertmannite was preserved, as described by Jonsson et al. (2005) and Schwertmann and Carlson (2005) (Fig. 3). A preserved morphology was found in Fe oxide aggregates also with Fe/S ratios >20 , which is much wider than the range of 4.6–8 characteristic for schwertmannite (Bigham et al., 1990; Jonsson et al., 2005).

The transformation product had a higher SO_4^{2-} retention capacity than goethite, as is evident from mass balance considerations. The mean Fe(III) content per sample was $1948\text{ }\mu\text{mol}$ ($\pm 58\text{ }\mu\text{mol}$). Complete transformation would have released up to $317\text{ }\mu\text{mol } \text{SO}_4^{2-}$, based on a stoichiometric ratio of $1.3/8$ ($\text{SO}_4^{2-}/\text{Fe}$) measured for the synthetic schwertmannite. Only a maximum of $20\text{ }\mu\text{mol } \text{SO}_4^{2-}$ was released and most SO_4^{2-} thus stayed on or within the solid phase. It was assumed that SO_4^{2-} was released from the schwertmannite structure but still bound to the newly formed Fe phase. Between 35% and 60% of SO_4^{2-} contained in schwertmannite can be adsorbed on the surface of schwertmannite (Bigham et al., 1990; Jonsson et al., 2005). A ‘typical’ goethite phase would only have retained around $39\text{ }\mu\text{mol } \text{SO}_4^{2-}$ ($1948\text{ }\mu\text{mol Fe}/50$), assuming a Fe/S ratio of 50 provided by Bigham et al. (1996b). With a surface of $115\text{ m}^2\text{ g}^{-1}$ as measured in a sample with almost complete transformation, the retention capacity for SO_4^{2-} increases only to $\sim 45\text{ }\mu\text{mol}$, assuming three sites nm^{-2} and a bidentate complex.

A redistribution of SO_4^{2-} can be argued for based on the observed changes in IR-absorption bands during transformation. Schwertmannite transformation coincided with the disappearance of ν_1 bands, which are indicative of distorted structural SO_4^{2-} tetrahedrons, and sustained and narrowed ν_3 bands (Fig. 4) (Jonsson et al., 2005; Nakamoto, 1997). Such a pattern, as observed for the sample 20°C , pH 5, $1\text{ mM } \text{SO}_4^{2-}$, is in agreement with SO_4^{2-} relocating from the schwertmannite structure to locations binding less distorted SO_4^{2-} tetrahedrons (Jonsson et al., 2005) at schwertmannite surfaces, i.e. weak outer sphere complexes. As the exact structure of schwertmannite is still discussed (Bigham et al., 1990; Majzlan and Myneni, 2005; Waychunas et al., 2001), it is not possible to clarify this point. A quantitative transfer, as necessitated by mass balance, would probably require a newly formed Fe phase with surface areas and properties similar to that of schwertmannite. This is not an unreasonable assumption considering the unaltered

morphology of the samples and a BET (Kr) surface area of $91.8 \text{ m}^2 \text{ g}^{-1}$ (34% transformation) and $115.2 \text{ m}^2 \text{ g}^{-1}$ (80–100% transformation). The conclusiveness of this information is limited, though, because surface areas of schwertmannite and goethite are variable (Cornell and Schwertmann, 1996).

Regardless of the uncertainty about the exact nature of the Fe phase formed, goethite was not the primary transformation product under the experimental conditions chosen. Instead, an X-ray amorphous Fe phase with a cloud-like morphology and a high capacity for SO_4^{2-} retention developed. The reasons for this finding are not easily identified. Rapid transformation at high pH values did not inhibit goethite formation in previous experiments (Schwertmann and Carlson, 2005). Most likely, the presence of SO_4^{2-} and DOC played a role, because earlier experiments were conducted in deionized water. This idea has some experimental support because the – already weak – IR bands characteristic of goethite further diminished when the SO_4^{2-} concentration was raised from 1 mmol L^{-1} to 20 mmol L^{-1} (electronic supplementary material, Fig. 1S). Addition of DOC had a similar effect and it may be expected that also other ions in the incubation solutions representing AMD would affect the transformation product through formation of ternary complexes and competition for exchange sites. Based on this observation it can be speculated that a more crystalline goethite, detectable by X-ray diffraction, would have formed in water even poorer in SO_4^{2-} . More experimentation at different concentrations of SO_4^{2-} would be required to confirm the influence of dissolved SO_4^{2-} on the nature of the transformation product. This was, however, beyond the scope of the present work, as it was intended to study schwertmannite transformation under geochemical conditions typical for environments polluted by AMD.

4.3. Implications for iron and acidity dynamics in AMD polluted waters

A low pH of 3, moderately high SO_4^{2-} and DOC concentrations, and low temperature effectively inhibited schwertmannite transformation in the experiments. Geochemical conditions of this kind are prevalent in AMD polluted lake sediments (e.g. Blodau and Peiffer, 2003; Kuesel, 2003; Peine et al., 2000; Regenspurg et al., 2004). Hence, it is not surprising that the transformation process

may need many years to be completed *in situ* (Peine et al., 2000), and advances much more rapidly in laboratory experiments using deionized water (Regenspurg et al., 2004; Schwertmann and Carlson, 2005). Vice versa, it is concluded that schwertmannite might rapidly transform *in situ* when geochemical conditions change, in particular when pore water pH values reach near-neutral levels and SO_4^{2-} is depleted. Given the strong dependency of transformation rates on these variables, schwertmannite will likely provide an effective pH buffer against increasing sediment pH, and decreasing SO_4^{2-} concentrations. This is an important conclusion because a near-neutral sediment pH is required for SO_4^{2-} reduction, Fe sulphide formation, and effective in-lake neutralization in these waters (Blodau and Peiffer, 2003; Kuesel, 2003). It would thus be expected that pH buffering by schwertmannite transformation will effectively counteract the pH-raising effect of organic substrate addition to AMD polluted lake sediments, and further stabilization of the pH in the acidic range would be expected, as long as the reservoir of schwertmannite is not depleted. Indeed, a pH increase proved difficult to accomplish in column experiments with Fe rich and acidic sediments (Knorr and Blodau, 2006) and was not sustained in lake enclosure experiments after organic substrates had been added and pore water pH had temporarily increased (Wendt-Pothoff et al., 2002).

The *in situ* development of an amorphous Fe phase may possibly also influence the internal acidification of surface waters by Fe reduction in the sediments and subsequent Fe(II) export to surface waters (Peine et al., 2000). The accessibility of Fe hydroxides for microbial reduction generally decreases with crystallinity and increases with surface area (Lovley and Phillips, 1988; Roden, 2003). The *in situ* formation of an amorphous Fe phase might thus contribute to the competitiveness of Fe reducers, and impede SO_4^{2-} reduction and Fe sulphide formation in sediments. Export of Fe(II) to surface waters would be promoted in this case and enhance in-lake acidification by Fe oxidation and precipitation of Fe(III) hydroxide in the surface waters.

Acknowledgements

We thank K. Söllner, S. Hammer and M. Haider for technical assistance, F. Heidelbach for access

and assistance with SEM and EDX, and S. Peiffer for critical comments.

Appendix A. Supplementary data

A document providing additional information on mineral synthesis, analytical methods, and further results not shown in the manuscript is available on-line. Supplementary data associated with this article can be found, in the online version, at doi:10.1016/j.apgeochem.2007.04.017.

References

Bigham, J.M., Schwertmann, U., Carlson, L., Murad, E., 1990. A poorly crystallized oxohydroxysulfate of iron formed by bacterial oxidation of Fe(II) in acidic mine waters. *Geochim. Cosmochim. Acta* 54, 2743–2758.

Bigham, J.M., Carlson, L., Murad, E., 1994. Schwertmannite a new iron oxyhydroxysulfate from Pyhäsalmi, Finland, and other localities. *Mineral. Mag.* 58, 641–648.

Bigham, J.M., Schwertmann, U., Pfaff, G., 1996a. Influence of pH on mineral speciation in a bioreactor simulating acid mine drainage. *Appl. Geochem.* 11, 845–849.

Bigham, J.M., Schwertmann, U., Traina, S.J., Winland, R.L., Wolf, M., 1996b. Schwertmannite and the chemical modelling of iron in acid sulfate waters. *Geochim. Cosmochim. Acta* 60, 2111–2121.

Blodau, C., 2004. Evidence for a hydrologically controlled iron cycle in acidic and iron rich sediments. *Aquat. Sci.* 66, 47–59.

Blodau, C., Peiffer, S., 2003. Thermodynamics and organic matter: constraints on neutralization processes in sediments of highly acidic waters. *Appl. Geochem.* 18, 25–36.

Cornell, R., 1987. Comparison and classification of the effects of simple ions and molecules upon the transformation of ferrihydrite into more crystalline products. *J. Plant Nutr. Soil Sci.-Z. Pflanzenernähr. Bodenkd.* 150, 304–307.

Cornell, R., Schwertmann, U., 1996. The Iron Oxides. VCH, Weinheim.

Fukushi, K., Miwa, S., Tsutomu, S., Nobuyuki, Y., Hikaru, A., Hodaka, I., 2003. A natural attenuation of arsenic in drainage from an abandoned arsenic mine dump. *Appl. Geochem.* 18, 1267–1278.

Gagliano, W.B., Brill, M.R., Bigham, J.M., Jones, F.S., Traina, S.J., 2004. Chemistry and mineralogy of ochreous sediments in a constructed mine drainage wetland. *Geochim. Cosmochim. Acta* 68, 2119–2128.

Jonsson, J., Persson, P., Sjoberg, S., Lovgren, L., 2005. Schwertmannite precipitated from acid mine drainage: phase transformation, sulphate release and surface properties. *Appl. Geochem.* 20, 179–191.

Kawano, M., Tomita, K., 2001. Geochemical modeling of bacterially induced mineralization of schwertmannite and jarosite in sulfuric acid spring water. *Am. Mineral.* 86, 1156–1165.

Knorr, K.H., Blodau, C., 2006. Experimentally altered groundwater inflow remobilizes acidity from sediments of an iron rich and acidic lake. *Environ. Sci. Technol.* 40, 2944–2950.

Kuesel, K., 2003. Microbial cycling of iron and sulfur in acidic coal mining lake sediments. *Water Air Soil Pollut.: Focus* 3, 67–90.

Lovley, D.R., Phillips, E.J.P., 1988. Novel mode of microbial energy metabolism: organic carbon oxidation coupled to dissimilatory reduction of iron or manganese. *Appl. Environ. Microbiol.* 45, 187–192.

Majzlan, J., Myneni, S.C.B., 2005. Speciation of iron and sulfate in acid waters: aqueous clusters to mineral precipitates. *Environ. Sci. Technol.* 39, 188–194.

Majzlan, J., Navrotsky, A., Schwertmann, U., 2004. Thermodynamics of iron oxides: Part III. Enthalpies of formation and stability of ferrihydrite (\sim Fe(OH)₃), schwertmannite (\sim FeO(OH)_{3/4}(SO₄)_{1/8}), and epsilon-Fe₂O₃. *Geochim. Cosmochim. Acta* 68, 1049–1059.

Meier, J., Costa, R., Smalla, K., Boehler, B., Wendt-Potthoff, K., 2005. Temperature dependence of Fe(III) and sulfate reduction rates and their effect on growth and composition of bacterial enrichments from an acidic pit lake neutralization experiment. *Geobiology* 3, 261–274.

Nakamoto, K., 1997. Infrared and Raman Spectra of Inorganic and Coordination Compounds. Wiley, New York.

Peak, D., Ford, R.G., Sparks, D.L., 1999. An in situ ATR-FTIR investigation of sulphate bonding mechanisms on goethite. *J. Colloid Interf. Sci.* 218, 289–299.

Peine, A., Tritschler, A., Kusel, K., Peiffer, S., 2000. Electron flow in an iron-rich acidic sediment – evidence for an acidity – driven iron cycle. *Limnol. Oceanogr.* 45, 1077–1087.

Regenspurg, S., Brand, A., Peiffer, S., 2004. Formation and stability of schwertmannite in acidic mining lakes. *Geochim. Cosmochim. Acta* 68, 1185–1197.

Roden, E.E., 2003. Fe(III) oxide reactivity toward biological versus chemical reduction. *Environ. Sci. Technol.* 37, 1319–1324.

Schwertmann, U., Carlson, L., 2005. The pH-dependent transformation of schwertmannite to goethite at 25 °C. *Clay Miner.* 40, 63–66.

Wallmann, K., Hennies, K., König, K.I., Petersen, W., Knauth, H.D., 1993. New procedure for determining reactive Fe(III) and Fe(II) minerals in sediments. *Limnol. Oceanogr.* 38, 1803–1812.

Waychunas, G.A., Myneni, S.C.B., Traina, S.J., Bigham, J.M., Fuller, C.C., Davis, J.A., 2001. Reanalysis of the schwertmannite structure and the incorporation of SO₄²⁻ groups: an IR, XAS, WAXY and simulation study. Conference-Abstract: Abstracts 11th annual V.M. Goldschmidt Conf. 2001 (<<http://www.lpi.usra.edu/meetings/gold2001/pdf/3849.pdf>>).

Wendt-Potthoff, K., Froemichen, R., Herzsprung, P., Koschorreck, M., 2002. Microbial Fe(III) reduction in acidic mining lake sediments after addition of an organic substrate and lime. *Water Air Soil Pollut.: Focus* 2, 81–96.

Yu, J.-Y., Heo, B., Choi, I.-K., Cho, J.-P., Chang, H.-W., 1999. Apparent solubilities of schwertmannite and ferrihydrite in natural stream waters polluted by mine drainage. *Geochim. Cosmochim. Acta* 63, 3407–3416.